ELSEVIER

Ceramics International 25 (1999) 409–414

CERAMICS
INTERNATIONAL

# Desorption of water during the drying of clay minerals. Enthalpy and entropy variation

A. Khalfi, P. Blanchart*

*Ecole Nationale Supérieure de Céramique Industrielle, ENSCI, 47 à 73 Avenue A.Thomas, 87065 Limoges Cedex, France*

Received 9 February 1998; accepted 13 May 1998

## Abstract

The purpose of this paper is to characterize the energy associated to the drying of three based clay raw materials containing mostly the minerals kaolinite, illite, and smectite, respectively. These natural clays, are commonly employed in many ceramic processes. Shaped samples were dried in a convection dryer at 55°C and 70°C, with an air humidity ratio ranging between 0.99 and 0.2. From the desorption isotherms, we have determined the enthalpy and entropy variations corresponding to the water desorption phenomena. They were calculated using the interpretation of the Gibbs free energy of the desorption mechanism, $H_2O_{adsorbed} \rightarrow H_2O_{free.liq.water}$. The behavior observed for shaped raw material containing kaolinite is similar to what is described in literature for kaolinite mineral. A maximum in binding heat of 17 kJ $mol^{-1}$ is observed for a complete monolayer coverage located between the layers of kaolinite clay. For shaped raw material containing smectite the behavior is fairly similar and the maximum in binding heat is about 18 kJ $mol^{-1}$. It corresponds to a situation for which 2/3 of the interlayer water is present. For shaped raw material containing illite, it was only possible to observe the beginning of the strong variation of $\Delta H°$ and $\Delta S°$ when the number of water layers on clay surface is low. © 1999 Elsevier Science Limited and Techna S.r.l. All rights reserved.

## 1. Introduction

The drying of a material consists in the removal of a liquid, often water. During this process, liquid molecules bonded to the material, in equilibrium with the surrounding atmosphere, can also be eliminated. In thermal drying, heat and gas flows accelerate the water separation from the material [1]. In the case of ceramic technologies, including clay as main paste component, the removal of water from shaped materials is an essential step of the process. The numerous physical and chemical phenomena linked to the water departure lead to dimensional variations of the material which may induce cracks [2]. Their formation depends on the dynamic conditions of heat and air flow [3,4] and on thermodynamic parameters such as temperature and water partial pressure.

The water removal from a shaped material involves two contributions, which are the departure of water and its transport forward the surfaces. Our approach in this paper is to determine for some clay based materials the energy change associated to the first contribution. Concerning the second aspect, we have chosen to proceed in steady state conditions with a carefully controlled air humidity. This procedure avoids any effect due to non controlled transport phenomena, during the water removal. In such conditions, the estimation of the energy to remove free and surface bonded water from a shaped material can be achieved. This parameter can be usefully exploited for modeling the water displacement when dynamic conditions of drying are employed [5].

The material behavior during water elimination is controlled by capillary water retained in the pores, by bonded water at the surface of the raw material grains and by crystallization water [6]. This latter, combined in the structure, vaporizes at higher temperatures than those generally used for drying (100°C) and is not concerned in this study.

The desorption behavior of a shaped material can be significantly different from that of the corresponding powder. Therefore, experiments were performed in a convection dryer equipment, especially designed to analyze shaped samples.

The raw materials studied are mainly phyllosilicates, i.e. clay minerals. In such compounds, the interaction

---

* Corresponding author.

PII: S0272-8842(98)00050-9

between water and material depends on the mineral type, on the arrangement of water molecules on surfaces and on the chemical nature of the cation which modifie the surface charge.

The three raw materials chosen for this study contain a percentage as high as possible of kaolinite, smectite and illite, respectively. The medium crystallised kaolinite (K), partially interstratified smectite (S) and common illite (I) are minerals commonly used in ceramic technologies. Since the purpose of this study is to obtain information on the behavior of natural raw materials, no purification of the starting material was performed. Moreover, in order to avoid surface hydrolysis, strong ion complexation or excessive water desorption, no further heat or chemical treatments were performed. These treatments highly modify the minerals comportment during the ceramic processes.

## 2. Raw materials analysis

Identification of the mineral phases present in the three raw materials has been made by powder X-ray diffraction using Co K$\alpha$ radiation. To improve the reliability, X-ray were performed in the $2.5 \leqslant 2\theta \leqslant 16°$ range on oriented powders obtained after settling from an aqueous suspension, in contact with air or after saturation with ethylene–glycol. The phase identification was achieved by comparison with literature data [7,8]. A chemical analysis by ICP was made on each sample. Results are presented in Table 1.

X-Ray diffraction spectrum on S powder presents peaks which are characteristic of quartz, calcite and smectite clay mineral. A large peak near 1.49 Å corresponds to the diffraction of the (060) plane present in dioctaedral minerals. On oriented samples, peaks at around 13–15.5 Å and at about 17 Å, before and after saturation with ethylene–glycol, respectively, are characteristic of the (001) plane of a swelling clay mineral. Furthermore, a small peak near 10 Å is characteristic of the illite/mica group. Lastly, kaolinite is also detected. After saturation with ethylene–glycol, the (001) peak intensity and the presence of another peak at 8.69 Å, which corresponds to (002) plane, are specific to an interstratified illite–smectite clay probably quite disordered.

The diffraction spectrum of I type clay presents a characteristic peak near 10 (before and after saturation with ethylene–glycol. Though a precise deconvolution is difficult to achieve in practice, the peak thickness which is larger than 0.2θ, suggests the presence of an illite mineral instead of a muscovite mica. However, we cannot exclude the presence of a complex peak corresponding to an illite and mica mix. Besides illite mineral, quartz and feldspar have also been detected.

The main peaks for K type raw material are well separated. They correspond to the dioctahedral kaolin subgroup, i.e. a true clay mineral. Peaks related to quartz and titanium oxides (rutile or anatase) are also observed. The correction of non silicate elements and an extensive separation of the finest grains, < 2 m, did not allows us to establish the presence of isomorphous substitution in the kaolinite structure.

From data in Table 1 and semi-quantitative analysis from X-ray spectra, it is possible to estimate the composition of each raw material. Results are reported in Table 2.

Table 1
Chemical compositions (weight %) of K, S and I raw materials

| | K | S | I |
|---|---|---|---|
| $SiO_2$ | 46.91 | 58.68 | 67.3 |
| $Al_2O_3$ | 33.39 | 15.87 | 19.9 |
| $Fe_2O_3$ | 1.66 | 3.72 | 2.37 |
| CaO | 0.5 | 1.54 | 0.04 |
| MgO | 0.17 | 2.52 | 0.82 |
| $K_2O$ | 0.01 | 1.85 | 6.01 |
| $Na_2O$ | 0.02 | 1.24 | 0.31 |
| $TiO_2$ | 1.89 | 0.75 | 0.03 |
| $Mn_2O_3$ | 0.01 | 0.07 | 0.03 |
| $P_2O_5$ | 0.08 | 0.09 | – |
| S | 0.18 | 0.08 | – |
| $SO_4$ | 0.07 | 0.12 | – |
| $CO_3$ | < 0.05 | 1.52 | – |
| Weight loss (700°C) | 15.11 | 11.95 | 3.19 |

## 3. Drying of raw materials

### 3.1. Thermodynamic analysis

Water desorption is associated with heat exchanges. Thanks to a thermodynamical approach, it is possible to evaluate the energy variation during drying.

Enthalpy and entropy variations of desorption can be calculated from isotherm desorption curves. The standard Gibbs free energy variation, $\Delta G_T°$, of the

Table 2
Mineralogical composition of (weight %) of K, S and I raw materials

| | K | S | I |
|---|---|---|---|
| Kaolinite | 88 | 8 | – |
| Illite | – | – | 60 |
| Illite–smectite | – | 79 | – |
| Quartz | 8 | 10 | 30 |
| Orthose | – | – | 8 |
| Albite | – | – | 2 |
| Calcite | trace | 2.5 | – |
| Gypse | trace | trace | – |
| Rutile | 2 | – | – |
| Pyrite | trace | trace | – |

transformation adsorbed water → free liquid water is given by:

$$\Delta G_T = \Delta H_T^\circ - T\Delta S_T^\circ = \overset{\circ}{\mu}_{\mathrm{H_2O(liq)}} - \overset{\circ}{\mu}_{\mathrm{H_2O(ads)}} \tag{1}$$

The standard chemical potentials of water, $\mu^\circ_{\mathrm{H_2O(liq)}}$ and $\mu^\circ_{\mathrm{H_2O(ads)}}$, are linked to the water partial pressure in the surrounding air atmosphere by:

$$\overset{\circ}{\mu}_{\mathrm{H_2O(liq)}} = \overset{\circ}{\mu}_{\mathrm{H_2O(g)}} + RT\ln(Pvs)_T \tag{2}$$

and

$$\overset{\circ}{\mu}_{\mathrm{H_2O(ads)}} = \overset{\circ}{\mu}_{\mathrm{H_2O(g)}} + RT\ln(Pv)_T \tag{3}$$

combining Eqs. (1)–(3) we obtain:

$$\Delta G_T^\circ = RT\ln(Pvs)_T/(Pv)_T \tag{4}$$

where $(Pv)_T$ and $(Pvs)_T$ are the atmosphere water partial pressures, in equilibrium at a given temperature $T$, in standard conditions with bounded and free liquid water, respectively. By combining Eq. (1) and Eq. (4) we obtain:

$$\ln(Pvs)_T/(Pv)_T = \Delta H_T^\circ/RT - \Delta S_T^\circ/R \tag{5}$$

Assuming that $\Delta H_T{}^\circ$ and $\Delta S_T{}^\circ$ do not depend on $T$ in a narrow temperature range, $\ln(Pvs)_T/(Pv)_T$ varies linearly with respect to $1/T$. The isosteric enthalpy and entropy variations of constant mass can be calculated from the isotherms for equal coverage or amount of water sorbed per unit mass of clay.

The standard enthalpy variation of the water desorption phenomenon at $T$, which is at constant pressure the heat of desorption, can be determined from the slope and the standard entropy variation can be estimated from the $(Pvs)_T/(Pv)_T$ value at $1/T=0$.

### 3.2. Experimental

The experimental equipment is presented in Fig. 1, and the major components are described in Ref. [9]. Its main characteristics are as follows: accuracy of the dry temperature of ±0.1°C (without any evaporation), humidity ratio controlled up to ±0.5%, possibility to monitor the air flow around the sample during weighing, sample mass measurement up to 100 g with an accuracy about 0.002 g.

The drying kinetics is strongly dependent on parameters related to sample texture, such as porosity and shape. In this study, to avoid excessive equilibrium time, some cylinders previously shaped (∅5 mm, $L$ ~10 cm) are stacked randomly to make a porous body.

Experimentally, the variations in sample weight were measured when the air humidity ratio varied linearly between 98% and 20% at a rate of 1% per hour. Two temperatures, 55 and 70°C, have been considered.

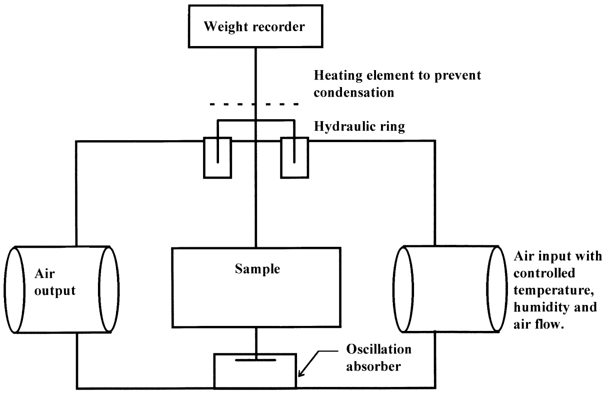

Fig. 1. Experimental equipment.

From isotherms, the isosteric characteristics corresponding to equal sample humidity have been obtained by a numerical method using a polynomial adjustment of symmetric intervals around each value.

### 3.3. BET analysis of desorption

Adsorption and desorption phenomena can be analyzed using the BET theory. Among the different hypothesis, the model considers the complete adsorption of successive layers [10,11]. This approach was already used to validate some surface area calculations based on structural characterization [12]. In the case of kaolinite mineral, it is agreed that interlayer water sheets form during the adsorption stage [13].

To reduce the discrepancy between adsorption and desorption phenomena, the measurements were performed at low sample humidity values, when the number of adsorbed water layers is very low. For such experiments, dry air was used to reduce $Pv/Pvs$ ratio down to 0.1.

The BET equation can be written under the form:

$$\begin{aligned} &Pv_T/Pvs_T/(Hs(1 - Pv_T/Pvs_T)) = \\ &Pv_T/Pvs_T(c-1)/(cHm) + 1/(cHm) \end{aligned} \tag{6}$$

where $Hs$ is the real sample water content and $Hm$ the sample water content for a monolayer coverage. The sample water content corresponds to the ratio between the bound water mass in the sample and the sample mass, after drying at 100°C. The $Hm$ value can be determined from the variation of Eq. (6) vs $(Pv)_T/(Pvs)_T$.

Results concerning S type raw material cannot be treated easily using the BET model, the hysteresis between adsorption and desorption being too strong (Fig. 2). For I type raw material, the humidity ratio

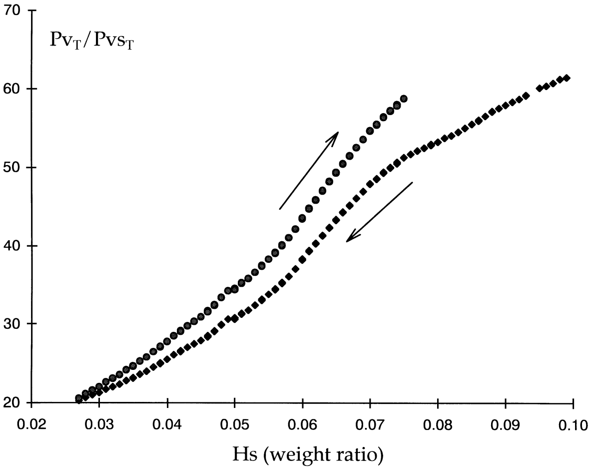

Fig. 2. Isotherms of water adsorption and desorption for S raw material at 55°C.

necessary for BET hypothesis are too low to be reached by our equipment. Therefore, only results concerning K type raw material were analyzed using the BET equation.

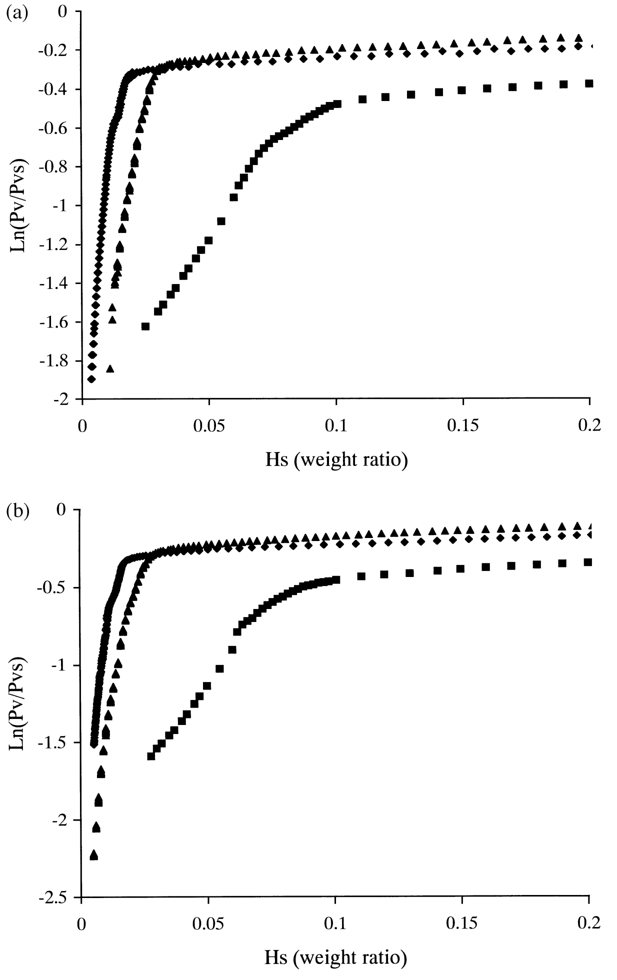

Fig. 3. Isotherms of water desoption for S (□), K (Δ) and I (◇) raw materials at 55° (a) and 70°C (b).

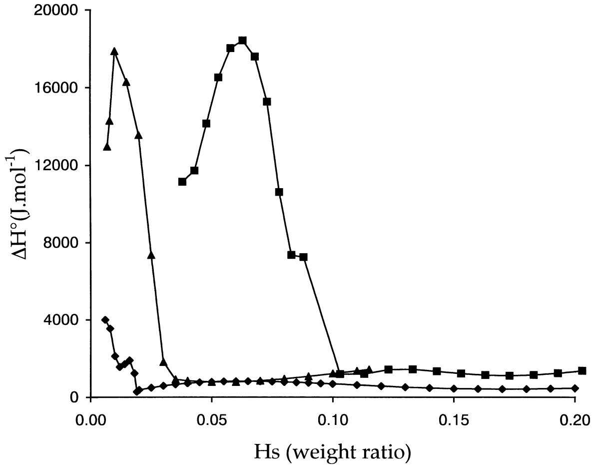

Fig. 4. $\Delta H°$ variation vs *Hs* for S (□), K (Δ) and I (◇) raw materials.

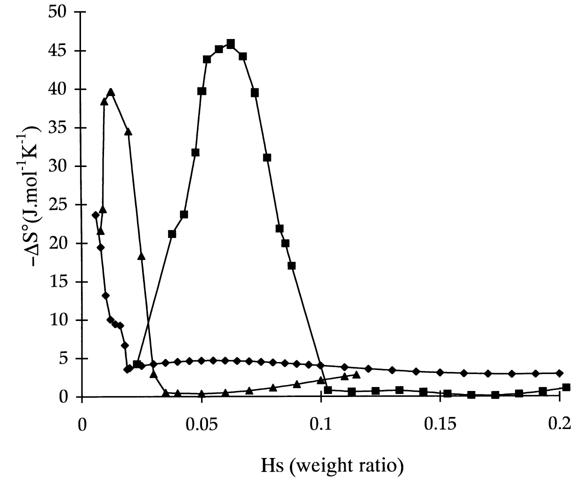

Fig. 5. $\Delta S°$ variation vs *Hs* for S (□), K (Δ) and I (◇) raw materials.

### 3.4. Results and discussion

Taking into account the hysteresis observed in the case of raw materials, we have chosen to consider only the desorption, which is representative of the drying phenomenon. The hysteresis was already explained as a result of the difference between the clay layer cohesion energy and the energy needed for the cation hydration [14].

Experimental isotherms obtained for S, K and I samples are presented in Fig. 3 at 55 and 70°C. $\Delta H_T$ and $\Delta S_T{}^{\circ}$ values were determined for various sample water contents, *Hs*, from the corresponding $(Pv)_T/(Pvs)_T$ ratio at the two temperatures using Eq. (5).

Results for the three clays are presented in Figs. 4 and 5. Three main stages can be pointed out on the $\Delta H°$ and $\Delta S°$ curves. At higher *Hs* value, $\Delta H°$ and $\Delta S°$ are fairly similar for the three clays and equal to 0.8 kJ $\text{mol}^{-1}$ and +5 J $\text{mol}^{-1}$ $\text{K}^{-1}$, respectively. When *Hs* decreases, a rapid increase in $\Delta H°$ and $\Delta S°$ is observed. The *Hs* value at which it starts depends on the type of clay and

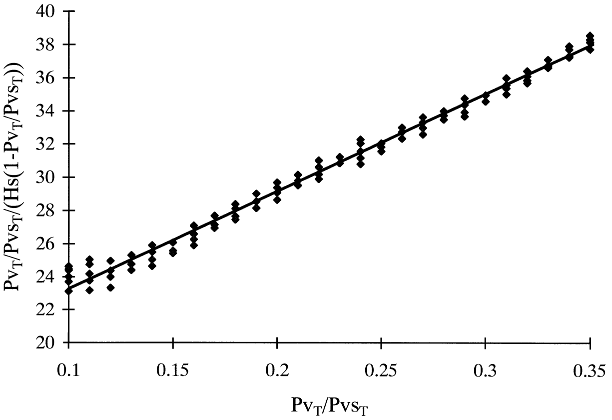

Fig. 6. BET plot for desoption of water on K raw material.

it is equal about 0.1 for S, 0.035 for K and 0.02 for I raw materials, respectively. For S and K type raw materials, $\Delta H^\circ$ and $\Delta S^\circ$ reach a maximum at *Hs* equal to 0.06 and 0.01, respectively and they decrease with *Hs*. For I raw material, it seems that this stage cannot be reached because of the very low values of sample humidity that it is necessary to attain during our experimental conditions.

Uncertainties on $\Delta H^\circ$ values can be estimated. The main error source is associated to the *Pv* value, the relative accuracy of *Pv*/*Pvs* is $\pm 0.005$. The temperature is controlled at $\pm 0.1$°C and samples were weighed with an accuracy of 0.001%. Taking into account all these uncertainties, $\Delta H^\circ$ values can be determined with an experimental accuracy of $\pm 0.8$ kJ mol$^{-1}$.

The strong variation of $\Delta H^\circ$ and $\Delta S^\circ$ observed during the second step of drying were already reported in the literature for kaolinite [15–17], smectite [17], montmorillonite [18–21] and illite minerals [14].

The $\Delta H^\circ$ value reported in the literature for kaolinite mineral is about 30 kJ mol$^{-1}$. In the present study, it is equal to 17 kJ mol$^{-1}$. This discrepancy can be attributed to the difference between pure kaolinite mineral and our K raw material. It can also correspond to a difference between water desorption and adsorption phenomena; our measurements were performed during desorption whereas those reported in the literature were often deduced from adsorption experiments.

During desorption of water bound on the surface of clay layer for S and I raw materials, there is an increase of $\Delta H^\circ$ equal to 18 kJ mol$^{-1}$ and 4 kJ mol$^{-1}$, respectively. A comparison can be made for S raw material with values reported for smectite and montmorillonite minerals, which range between 6 and 30 kJ mol$^{-1}$, depending on authors. For I raw material, the reported data range between 3 and 9 kJ mol$^{-1}$, which is close to our result.

The BET plot for K raw material is presented in Fig. 6 for air humidity below 0.35. This plot is almost a straight line, in the humidity range 0.1–0.35, with a positive intercept. The calculated *Hm* value for a monolayer coverage is 0.012. It is close to the sample water content for which $\Delta H^\circ$ and $\Delta S^\circ$ present a maximum (Figs. 4 and 5). Consequently, the maximum of $\Delta H^\circ$ and $\Delta S^\circ$ for our K raw material could correspond to a monolayer coverage. Such a maximum in adsorption or desorption heat, associated to the presence of one complete layer of water between kaolinite clay layer was already mentioned in the literature [15,16,19].

It can be also noticed that the start of the increase of $\Delta H^\circ$ and $\Delta S^\circ$ is observed for K raw material at a sample water content near 0.035, which corresponds to about three times the humidity associated to a monolayer coverage of clay layers. This result suggest that $\Delta H^\circ$ and $\Delta S^\circ$ increase when a third layer of water is formed. This assumption is in agreement with the generally admitted hypothesis that three layers of water are trapped between clay layer surfaces [4].

For K raw material, the behavior during progressive drying under decreasing water vapor pressure can be described as follows:

- For the highest sample water content, desorption corresponds to departure of water molecules which are weakly bounded to the particle surfaces. The bonding heat is weak and quite constant. The entropy of this bound water is slightly lower than that of free water.
- For a sample water content lower than 0.035, the eliminated water corresponds to the desorption of the water bonded between clay layers. The elimination of the first two layers corresponds to an increase of the desorption entropy, associated to an increase of the bound heat. Simultaneously, the entropy of the bound water decreases strongly.
- The progressive elimination of the last water layer located between clay layers is associated to a decrease in the water desorption heat and to an increase in the bound water entropy.

For S raw material, the behavior is quite different. The beginning of $\Delta H^\circ$ and $\Delta S^\circ$ increase and the maximum of $\Delta H^\circ$ correspond respectively to 0.103 and 0.064. The phenomenon observed in this range of sample water content should correspond to the desorption of the clay interlayer water. It seems that the maximum of the desorption heat and the minimum of the bound water entropy correspond to the elimination of 2/3 of the interlayer water, which is different from the 1/3 value observed for K sample. A small accident exists on the $\Delta H^\circ$ vs *Hs* curve at about 0.085 and its origin is still unknown.

## 12. Conclusion

This study was devoted to the characterization of the drying behavior of natural clays, kaolinite, illite and smectite based raw materials. The experiments performed at 55 and 70°C allowed us to characterize the desorption behavior of water bound on particle surfaces and between clay layers.

For shaped K raw material, a maximum of desorption heat, 17 kJ $mol^{-1}$, is observed when a complete monolayer coverage is located between the kaolinite clay layers. Beyond the maximum, the incomplete layer results in a desorption heat reduction. For shaped S raw material, the maximum of desorption heat is 18 kJ $mol^{-1}$ of bound water. At this point, the clay water content is higher than for kaolinite clay, although 2/3 of the clay interlayer water is present. For I shaped raw material, the very low air humidity ratio required to entirely characterize the interlayer water was not possible to attain, due to equipment limitations. Nevertheless, it was possible to observe the beginning of a strong variation of $\Delta H^\circ$ and $\Delta S^\circ$, for water content lower than 0.02, when the number of water layers on clay surface is low. The next stage will be to correlate these different water departure with the mechanical strength of the final product.

## References

[1] E. Krause, Le séchage en céeramique, principes et techniques, Ed. Septima, Paris, 1977.

[2] J.E. Funk, Simultaneous weight loss and shrinkage of clays, Ceram. Bull. 53 (1974) 450–453.

[3] R. Hermann, Drying of tableware, Ceramic Monographs, Supplement to Interceram 38 (2) (1989) No. 1.5.3.

[4] Chemistry of clays and clay minerals, in: A.C.D. Newman (Ed.), Mineralogical Society, Monograph No. 6, Longman Scientific & Technical, London, 1987.

[5] A. Escardino, M.A. Gallego, C. Filiu, A. Barba, E. Sanchez, Drying of ceramic material, Br. Ceram. Trans. 92 (1993) 197–202.

[6] J.B. Dixon, S.B. Weed, Minerals in Soils Environnents, 2nd Edition, Soil Sci. Society of America, Madison, USA, 1989.

[7] J. Thorez, Phyllosilicates and minerals, a laboratory handbook for their X-rays analysis, Editions G. Lelote, Dison, Belgium, 1975.

[8] H.P Klug, L.E. Alexander, X-ray diffraction procedures of polycristalline and amorphous materials, John Wiley & Sons, New York, 1974.

[9] F. Weber, J.M. Gaillard, P. Blanchart, The drying of clay minerals and mixed clay minerals, J. Mat. Sci. 30 (1995) 2319–2324.

[10] R.W. Mooney, A.G. Keenan, L.A. Wood, Adsorption of water vapor by montmorillonite. I. Heat of sorption and application of BET theory, J. Am. Chem. Soc. 74 (1952) 1367–1374.

[11] R.R. Dyal, S.B. Hendricks, Total surface of clay in polar liquids as a characteristic index, Soil Sci. 62 (1950) 421–432.

[12] M.D. Heilman, D.L. Carter, C.L. Gonzalez, The ethylene glycol monoethyl ether technique for determining soil-surface area, Soil. Sci. 100 (1965) 409–413.

[13] J.J. Jurinak, Multilayer adsorption of water by kaolinite, Soil Sci. Soc. Am. Proc. 27 (1963) 269–272.

[14] R.Sh. Mikhail, N.M. Guindy, S. Hanafi, Vapor adsorption on expanding and nonexpanding clay minerals J. Coll. Int. Sci. 70 (1979) 282–292.

[15] I.G. Poliakova, Yu. Tarasevich, Adorption—calorimetric measurements on the state of water close to hydrophobic surfaces, Kolloidnyi Zhurnal 53 (1991) 386–391.

[16] I.G. Poliakova, Yu. Tarasevich, Heat and entropy of adsorption of water on Li-kaolinite, Dokjlady Akademii Nauk SSSR 236 (September) (1977) 681–684.

[17] J. Fripiat, J. Cases, M. Francois, M. Letellier, Thermodynamic and microdynamic behavior of water in clay suspensions and gels, J. Colloid Interface Sci. 89 (1982) 378–400.

[18] M.H. Fu, Z.Z. Zhang, P.F. Low, Changes in the properties of a montmorillonite–water system during the adsorption and desorption of water: hysteresis, Clays and Clays Minerals 38 (1990) 485–492.

[19] Z.Z. Zhang, P.F. Low, Relation between the heath of immersion and the initial water content of Li, Na, and K-montmorillonite, J. Colloid Interface Sci. 133 (1989) 461–472.

[20] G. Dios Cancela, F.J. Huertas, E. Romero Taboada, F. Sanchez-Rasero, A. Hernandez Laguna, Adsorption of water vapor by homoionic montmorillonites. Heats of adsorption and desorption, J. Colloid Interface Sci. 185 (1997) 343–354.

[21] Yuji Torikai, Seichi Sato, Hiroshi Ohashi, Thermodynamic properties of water in compacted sodium montmorillonite, Nuclear Technology 115 (1996) 73–80.